JOURNAL OF AIRCRAFT
Vol. 46, No. 3, May–June 2009

Engineering Notes

ENGINEERING NOTES are short manuscripts describing new developments or important results of a preliminary nature. These Notes should not exceed 2500 words (where a figure or table counts as 200 words). Following informal review by the Editors, they may be published within a few months of the date of receipt. Style requirements are the same as for regular contributions (see inside back cover).

Flowfield of a Forward-Facing Shaped-Charge Cavity

R. Rifki* and A. Ahmed†
Auburn University, Auburn Alabama 36849

DOI: 10.2514/1.38125

Introduction

THE air-dispensed grenades submunitions are ribbon-stabilized and are designed to descend vertically and impact the target at low angles of attack at a terminal velocity with minimum oscillations (Fig. 1). During a series of wind-tunnel tests on a full-scale grenade model with a variety of ribbons, four distinct stability characteristics were observed, ranging from exponentially damped oscillations, partly damped small-amplitude oscillations, highly amplified oscillations, and locking on to a different angular attitude with superimposed low-amplitude oscillations [1].

A postlaunch time history of the grenade model deployed at 90 deg to the direction of descent during the wind-tunnel tests is shown in Fig. 2. Because the model is constrained from oscillating in the vertical plane, oscillations represent yawing motion in horizontal plane only. In one case, the oscillations die quickly and the grenade approaches an equilibrium condition after release, and in the second case, oscillations continue to amplify after the grenade locks on to a different mode altogether. Figure 2 also shows that some ribbons are successful in damping the oscillations, whereas others contribute to instability introduced by wake–ribbon interactions.

Air-launched grenades are short-aspect-ratio bluff bodies with a well-defined singular point (stagnation point) that is detached and lies at a certain distance ahead of the body during descent. Because of the geometry of the shaped charge, a grenade acts like a forward-facing cavity, with some exchange of fluid between the cavity and the surrounding. Uniqueness of the primary singular point yielding simple topology has been analytically established for low Reynolds numbers in the past [2] and is similar to forward-facing cavities investigated experimentally and numerically for steady hypersonic flow conditions [3]; however, no downstream effects have been documented. The objective of the present investigation, therefore, was to understand the mechanism of fluid dynamics interactions between the detached singular point, flow inside of the cavity, and the flow in the near wake of a short nonstreamlined body with abrupt leading and trailing ends, such as the air-launched grenade.

Presented as Paper 0670 at the 44th AIAA Aerospace Science Meeting and Exhibit, Reno, NV, 9–12 January 2006; received 17 April 2008; accepted for publication 10 March 2009.

*Graduate Research Assistant, Aerospace Engineering Department. Student Member AIAA.

†Associate Professor, Aerospace Engineering Department. Associate Fellow AIAA.

Experimental Setup

A full-scale grenade model with a shaped-charge cavity configuration was used in this investigation. The model was made from a clear acrylic stock and polished to obtain transparency for flow visualization and particle image velocimetry (PIV) measurements. Side and front views of the model are shown in Fig. 3.

Tests were conducted in the Auburn University water tunnel with a 45×45 cm cross section. The water tunnel has a maximum velocity of 1 m/s and is equipped with additional top walls for open- or closed-surface operations. Reynolds numbers based on the diameter of the model ranged from 7000 to 43,000.

The model was mounted from the rear on a straight tube connected to a C-strut that rested on top of the tunnel sidewalls. The support tube was also used for injection of fluorescent dye for flow visualization and seed particles for PIV measurements inside the cavity. Details of the model support system are shown in Fig. 4.

Hydrogen-bubble probes with single and multiple platinum wires were used for flow visualizations. Bubble probes were mounted on a separate 2-degree-of-freedom traversing system for precise positioning. The quantity and size of the bubbles was controlled by a set of variable voltage power supplies (20–60 V). The centerline planes of the models were illuminated with the help of an OZ Optics laser light sheet generator attached to a 5 W argon-ion laser. Fluorescent dye was also injected inside the cavity to examine internal flow structures. A Sony charge-coupled device camera was used to capture images that were recorded in real time on a JVC professional VCR.

A Dantec Dynamics Flow Map PIV system, consisting of 50 mJ dual-pulsed YAG lasers and a 1.1×1.1 k cross-correlation camera,

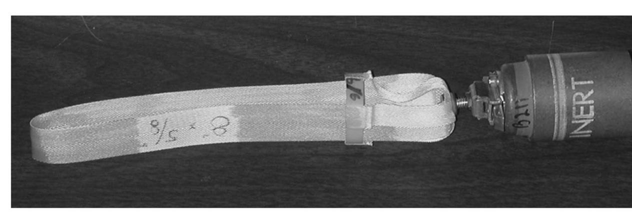

Fig. 1 Ribbon-stabilized air-launched grenade.

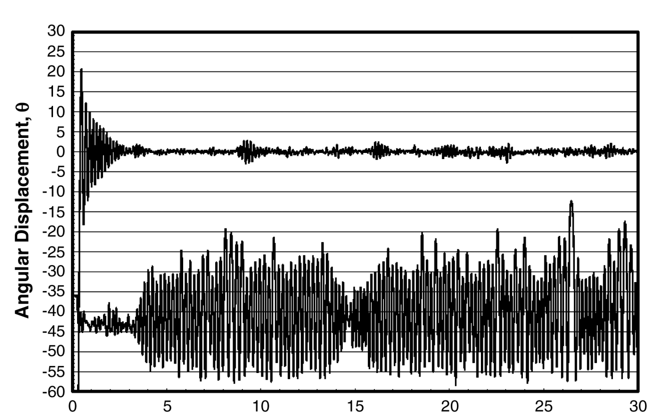

Fig. 2 Time history of damped (upper trace) and amplified (lower trace) oscillations.

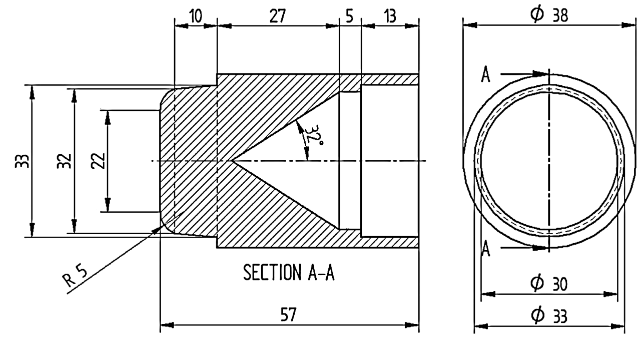

Fig. 3 Details of the forward-facing shaped-charge cavity model (dimensions in millimeters).

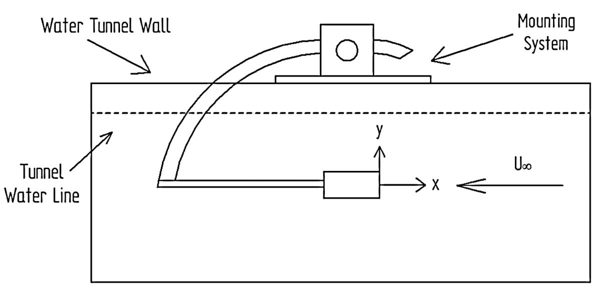

Fig. 4 Water-tunnel model support system.

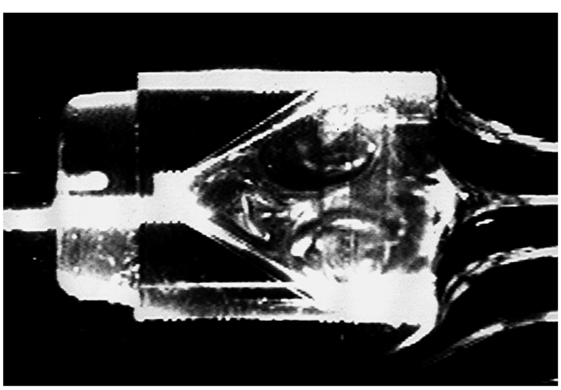

Fig. 5 Flow visualization of the shaped-charge cavity (flow from right to left).

was used for velocity measurements. Flow statistics were computed from a set of 1000 pairs of images recorded for each test condition using cross-correlation and adaptive-correlation techniques on a 32×32 pixel interrogation window with 50% overlap. Uncertainty estimates of the mean velocities were found to be less than 4% for the range of Reynolds numbers tested.

Fluctuation of the singular point and its correlation with the flowfield downstream of the model were measured using a TSI, Inc., IFA 300 constant-temperature anemometer system and two hot-film probes. The upstream probe was positioned close to the lip of the cavity, and the downstream probe was located at a distance of 2 diameters from the rear end of the model. The data rate was 100 Hz, and the time histories consisting of 8000 points were postprocessed using MATLAB software.

Results and Discussion

A flow visualization image is shown in Fig. 5. Here, the illumination is provided by a vertical laser light sheet that is perpendicular to the optical axis of the camera. The freestream is marked with horizontal sheets of hydrogen bubbles from three platinum wires, and the flow inside the cavity is visualized with the help of fluorescent dye injected directly in the cavity.

Analysis of video records of flow visualization revealed complex fluid dynamics interactions in the entire flowfield. The whole-field flow visualization using a combination of horizontal and vertical hydrogen bubble sheets and fluorescent dye indicated that although in one plane, the outside fluid continued to be intermittently entrained, in the other plane, fluid was being ejected. In a related investigation on straight cavities, it was determined that the amount of entrainment and ejection was cavity-volume-dependent and Reynolds-number-dependent [4]. PIV results of the entrainment and ejection of flow from the cavity are presented in Fig. 6.

To understand the behavior of the primary singular point, tests were repeated for one of the models with the front end sealed. The model thus looked like a short-aspect-ratio cylinder axially facing the flow. The flow visualization results presented in Fig. 7 clearly show that the attachment streamlines were deflected further upstream of the cavity when its opening was sealed.

Flow visualization of the wake also revealed the coalescence of eddies emanating from and near the reattachment point with the coherent structures of the wake. Unsteadiness in the flow, however, was found to be less severe when the face of the cavity was sealed. The primary singular point was also found to be very sensitive to freestream disturbances that caused unconstrained large-scale oscillations in the wake. Similar oscillations have been reported in the flowfield of axisymmetric cavities [5].

The corresponding PIV measurements of the same flow presented in Fig. 8 clearly show a larger region of separation near the lip of the closed cavity. Also evident is the larger detachment distance of the bifurcating streamline in the plane of symmetry of the closed cavity compared with the open cavity. The location of the bifurcating streamline and primary singular point was determined from PIV results using $u = 0$ criterion along the $y = 0$ line and matched well with the flow visualization results.

A simplified topological illustration based on these observations is presented in Fig. 9. It may, however, be noted that the presence of

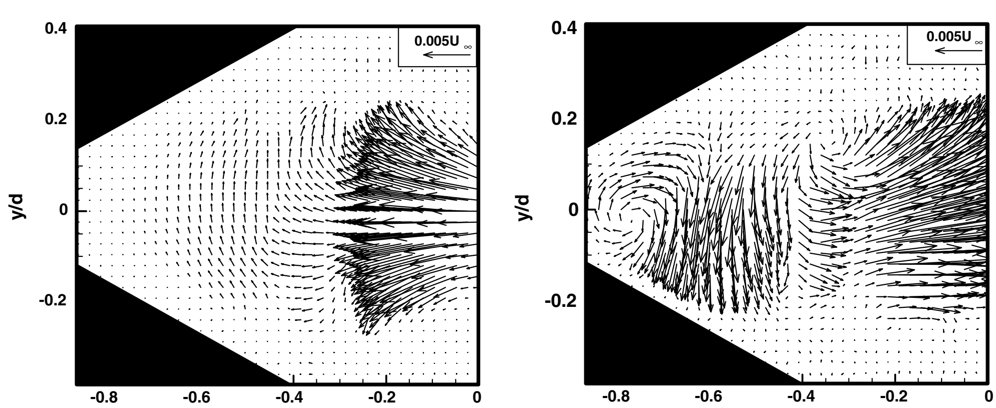

Fig. 6 Entrainment of external fluid inside the cavity (left) and ejection of fluid from the cavity (right).

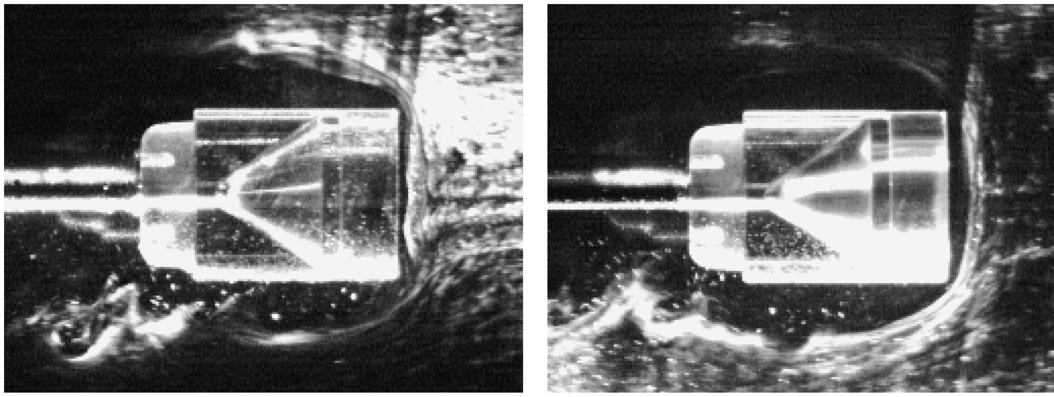

Fig. 7 Flow visualization of external flow in the forward region of the cavity; open cavity (left) and cavity with sealed front end (right).

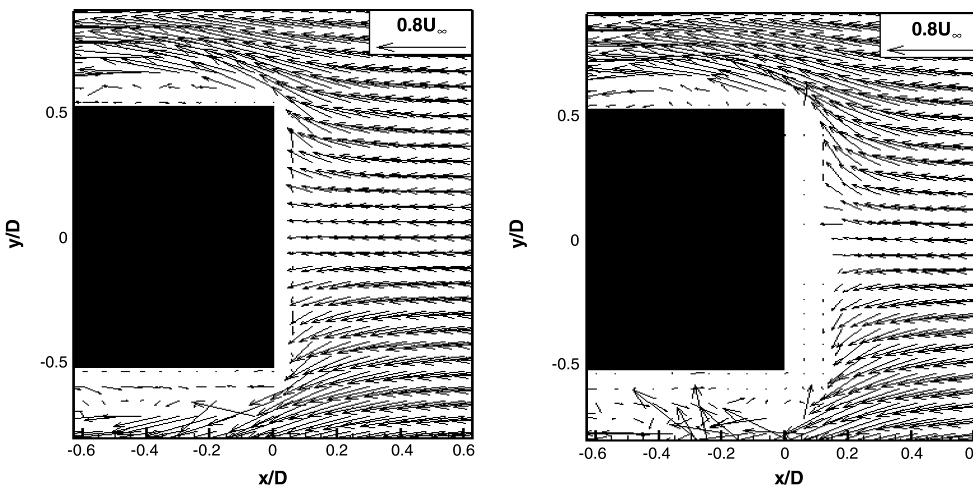

Fig. 8 Vector map of flow around the cavity model; open cavity (left) and cavity with sealed front end (right).

nodes, half-nodes, and half-saddles is intentionally ignored in describing the key features of the flow [6].

An important feature of the flow is the formation of primary singular point S_1, as shown in Fig. 9a. As more fluid is entrained, secondary structures appear in the cavity and $S1$ connected to the bifurcating streamline movies upstream. This is followed by the formation of a secondary singular point $S2$ (Fig. 9b). Flow inside the cavity remains unsteady and the structures continue to swell and shrink radially because of the shape of the cavity and interactions with the side walls. Furthermore, motion of the flow structures

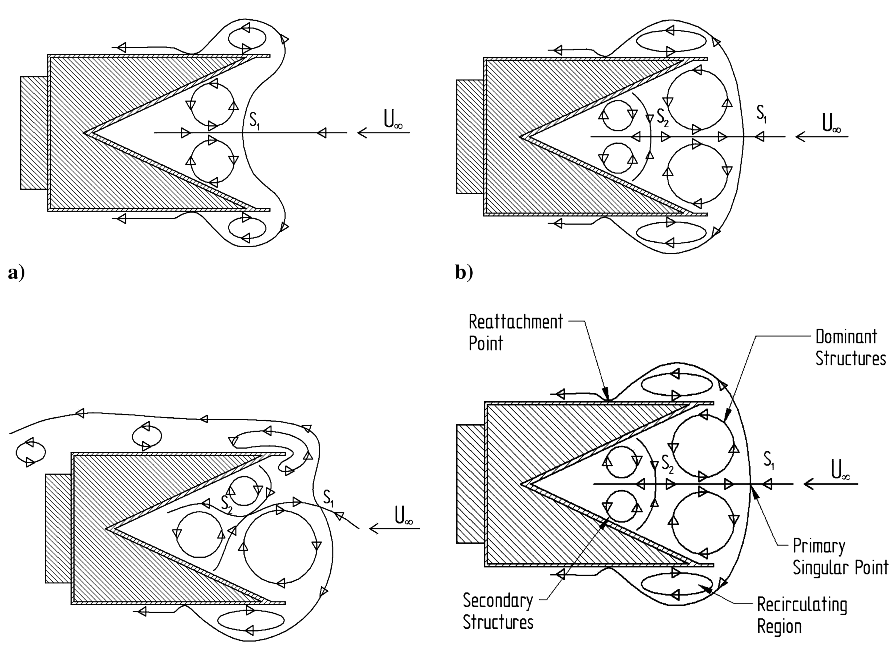

Fig. 9 Simplified topological illustration of the flow.

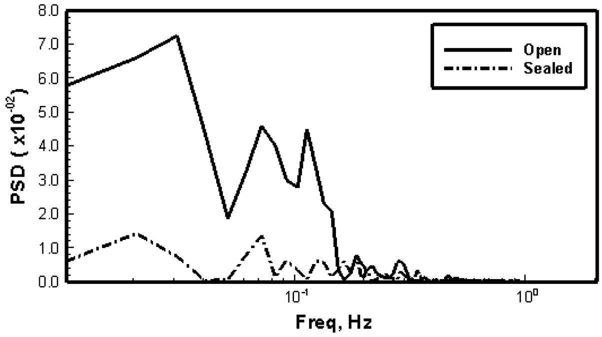

Fig. 10 Power spectra of the flow near the front face of the cavity at $Re_d = 35,000$.

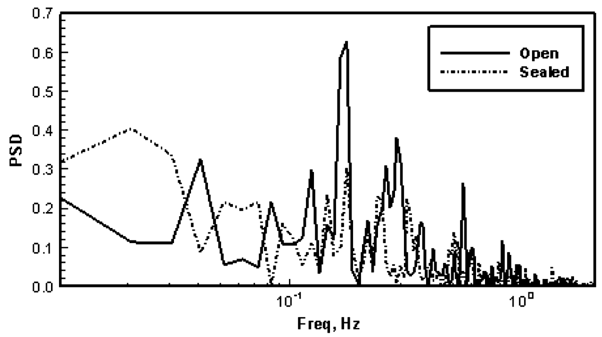

Fig. 11 Wake power spectra of the sealed and open cavities at $Re_d = 35,000$.

resembles a marble moving in a combination of circular and elliptical trajectories in a cup. As more fluid is entrained, the structures closer to the lip of the cavity are intermittently squeezed and expelled and, after merging with the recirculating eddy in the reattachment region, are puffed out downstream toward the wake (Fig. 9c). The breathing of the cavity thus interacts with the primary singular point that becomes unsteady and consequently imposes additional strain on the entire flowfield extending to the wake. This is similar to the observations of Ericsson [7] for unsteady cavity flow. Flow later takes the form presented in Fig. 9d before beginning a new cycle.

The power spectrum of the signals from a hot-film sensor placed near the front of the model show contrasting difference in the level of power spectral density for the two cases (Fig. 10).

Flow oscillations in the vicinity of the primary singular point with a dominant peak at 0.18 Hz were also detected in the power spectrum of the wake probe. The cross spectrum revealed subharmonic interactions, confirming the flow visualization results. Dominant frequency in the wake was measured (and confirmed with auto-correlation) and resulted in the average wake Strouhal number of 0.17 based on the diameter of the model. The wake power spectra of the sealed and open cavities presented in Fig. 11 clearly indicate higher power spectral density levels and the presence of additional scales due to the cavity.

Conclusions

The singular-point oscillations and wake coupling observed in this investigation fall in the category of classic absolute instability case and it is concluded that detached singular points (of attachment) are susceptible to perturbations in the flow and their streamwise spatial location is Reynolds-number-dependent. Flow inside of a shaped-charge cavity consists of structures that entrain outside fluid and are ejected randomly from the cavity. After leaving the cavity, these structures reside in the reattachment region before shedding in the wake. A simplified topology of the flow is presented. Spectral contents of the hot-film probe data showed higher energy peaks at the lower wave numbers, indicating subharmonic interactions.

Acknowledgments

This work was supported by the U.S. Army Redstone Arsenal, Huntsville, Alabama, with Lamar Auman as the Technical Monitor.

References

[1] Auman, L. M., and Dahlke, D., "Aerodynamic Characteristics of Ribbon-Stabilized Grenades," AIAA Paper 2000-0270, 2000.

[2] Dorrepaal, J. M., O'Neill, M. E., and Ranger, K. B., "Axisymmetric Stokes Flow Past a Spherical Cup," *Journal of Fluid Mechanics*, Vol. 75, 1976, pp. 273–286.
doi:10.1017/S0022112076000219

[3] Engblom, W. A., Yuceil, B., Goldstein, D. B., and Dolling, D. S., "Experimental and Numerical Study of Hypersonic Forward-Facing Flow," *Journal of Spacecraft and Rockets*, Vol. 33, No. 3, 1996, pp. 353–359.
doi:10.2514/3.26767

[4] Rifki, R., "Flow Around Axisymmetric and Two-Dimensional Forward Facing Cavities," M.S. Thesis, Department of Aerospace Engineering, Auburn Univ., Auburn, AL, 2006.

[5] Gharib, M., and Roshko, A., "The Effect of Flow Oscillations on Cavity Drag," *Journal of Fluid Mechanics*, Vol. 177, 1987, pp. 501–530.
doi:10.1017/S002211208700106X

[6] Hunt, J. C. R., Abel, C. J., Peterka, J. A., and Woo, H., "Kinematical Studies of Flows Around Free or Surface Mounted Obstacles; Applying Topology to Flow Visualization," *Journal of Fluid Mechanics*, Vol. 86, 1978, pp. 179–200.
doi:10.1017/S0022112078001068

[7] Ericsson, L. E., "Asymmetric Unsteady Flow in Forward Facing Cavities," *Journal of Spacecraft and Rockets*, Vol. 15, No. 6, 1978, pp. 321–327.
doi:10.2514/3.57322